CrossMark

ORIGINAL PAPER

Increased Gal-9 and Tim-3 expressions during liver damage in a murine malarial model

Siyu Xiao[1,2] · Jinfeng Liu[1,2] · Shiguang Huang[3] · Fangli Lu[1,2]

Abstract Malaria has been one of the most devastating tropical parasite infectious diseases popular around the world. Severe malaria is characterized by multiple organ dysfunctions, especially liver damage. However, the mechanisms of malarial liver injury remain to be better clarified. In this study, Kunming mice inoculated intraperitoneally (i.p.) with 10^6 *Plasmodium berghei* ANKA (*Pb*ANKA)-infected red blood cells (iRBCs) were investigated at days 5, 10, 15, and 20 post-infection (p.i.) to elucidate the profiles of T-cell immunoglobulin and mucin domain-3 (Tim-3) and its ligand galecin-9 (Gal-9) in the development of liver injury. The histopathology of livers and spleens from *Pb*ANKA-infected mice were observed, the parasite burdens of the livers and spleens using quantitative real-time PCR (qRT-PCR), Tim-3- and Gal-9-positive cells in the livers and spleens using immunohistochemical staining, and the mRNA levels of Tim-3, Gal-9, and cytokines in both the livers and spleens using qRT-PCR were examined. Our results showed that parasite burdens in the livers and spleens were significantly increased with time after *Pb*ANKA infection. Histological scores of both the liver and spleen tissues were significantly increased with time; the numbers of Tim-3- and Gal-9-positive cells were significantly increased in both the livers and spleens using immunohistochemical staining, and the mRNA levels of Tim-3 and Gal-9 in the livers and spleens were also significantly increased after infection. Our data suggests that the increase of Tim-3/Gal-9 expressions may play an important role in the liver damage during *P. berghei* infection.

Keywords *Plasmodium berghei* · Liver · Tim-3 · Gal-9 · Mice

Introduction

Malaria has been one of the most devastating tropical parasite infectious diseases popular around the world. Severe malarial syndromes include severe anemia, hyperparasitemia, cerebral malaria, acute respiratory distress, and clinical jaundice, with the brain, lungs, kidney, and liver all variously affected (WHO 2010). Malaria-associated liver dysfunction is commonly observed in severe malaria, both in adult and pediatric patients (Whitten et al. 2011; Anand and Puri 2005), which is a heterogeneous pathology with variable severity, as symptoms range from mild changes in liver function tests to severe liver failure. Malaria infection can lead to an extremely complicated series of immune response in the liver, and histopathological findings such as portal mononuclear cell infiltration are observed in varying degrees (Murthy et al. 1998). However, the mechanisms behind it are largely unknown.

The T-cell immunoglobulin and mucin domain (Tim) family is a relatively newly described group of molecules with a conserved structure and important immunological functions (Li et al. 2013). It has been reported that after peroral infection of *Toxoplasma gondii*, genetically susceptible C57BL/6 mice develop an unchecked Th1 response associated with the

✉ Shiguang Huang
thshg@126.com

✉ Fangli Lu
fanglilu@yahoo.com

1 Department of Parasitology, Zhongshan School of Medicine, Sun Yat-sen University, Guangzhou 510080, Guangdong, China

2 Key Laboratory of Tropical Disease Control (Sun Yat-sen University), Ministry of Education, Guangzhou 510080, Guangdong, China

3 School of Medicine, Jinan University, Guangzhou 510632, Guangdong, China

development of small intestinal immunopathology and exhibit increased frequencies of Tim-3^{+} cells in spleens and mesenteric lymph nodes (Berrocal Almanza et al. 2013). Galectin-9 (Gal-9) is a member of the galectin family that selectively binds to β-galactoside (Wada and Kanwar 1997), modulates immune responses by interaction with Tim-3, induce Th1 cell apoptosis to dampen Th1 immunity, and induce peripheral tolerance. The Tim-3/Gal-9-signaling pathway plays a critical role in the homeostasis of hepatic NKT cells through activation-induced apoptosis and secondary proliferation and contributes to the pathogenesis of nonalcoholic fatty liver disease (Tang et al. 2013). So far, the role of Tim-3/Gal-9 interaction in controlling inflammatory lesions caused by malarial infection has little to be explored. In the present study, we used a *Pb*ANKA-infected mouse model to investigate the immune response and malaria-associated liver injury in mice, focusing on the effects of Tim-3/Gal-9 expression on the process of *Pb*ANKA infection in vivo, thus providing experimental evidence for the prevention and treatment of malaria-associated liver injury.

Materials and methods

Mice and experimental infections

Female Kunming (KM, outbred) mice (6–8 weeks old) and *Plasmodium berghei* ANKA (*Pb*ANKA) were used throughout the study. A total of 50 mice were included, in which 46 mice were injected intraperitoneally (i.p.) with 10^6 *Pb*ANKA-infected red blood cells (iRBCs) and 4 mice were injected with equal volume of phosphate buffered saline (PBS) as negative controls. Mortality was monitored daily. There were 24 *Pb*ANKA-infected mice, in which 6 were sacrificed by CO_2 asphyxiation for examination at 5, 10, 15, and 20 days p.i., respectively, and the remaining 22 *Pb*ANKA-infected mice were used for survival and parasitemia observation. All experiments were performed in compliance with the requirements of the Animal Ethics Committee at Sun Yat-sen University.

Parasitemia

For assessment of parasite multiplication in mice infected with *Pb*ANKA, malaria parasitemia was monitored daily by Giemsa-stained thin blood smears of tail blood. Erythrocyte counts were performed with a hematocytometer, and more than 1000 RBCs were counted by light microscopy (×100) to determine the percentage of parasitized cells.

Histopathology

For histopathological analysis, liver and spleen tissues from mice infected with *Pb*ANKA were fixed in 10 % neutral-buffered formalin (Guangzhou Chemical Reagent Factory, China) for 48 h, dehydrated, embedded in paraffin, sectioned (4 μm), and stained with hematoxylin and eosin (H&E; Sigma-Aldrich) for evaluation of pathologic changes. Sections of liver and spleen tissues from uninfected mice treated with PBS were used as negative controls.

The pathological analyses of the sections were blinded for semi-quantitative histopathological analysis under a microscope. Changes in the histopathological features in liver and spleen tissues were classified based on the severity of four histological criteria: architecture loss, sequestration of parasitized red blood cells (PRBCs) in microvessels, and pigment deposition and inflammation (Fazalul Rahiman et al. 2013; Viriyavejakul et al. 2014). The histopathological changes were graded on a scale as follows: nil (0), partial loss (1), moderate loss (2), and total loss (3). The highest possible total score was 12 (4 histological criteria×3 as highest scale). Score 0 meant no histopathological change and score 12 referred to the most severe histopathological change (Fazalul Rahiman et al. 2013). Overall liver and spleen tissues were analyzed at a magnification of ×100 under a light microscopy by counting 10 fields of each section from each mouse in each group. All the analyses were performed by two researchers.

Immunohistochemical staining for Tim-3 and Gal-9 in the livers and spleens

Immunohistochemistry was carried out using the streptavidin-biotin-peroxidase complex (SABC) method. For immuno-histopathological examination of Tim-3 and Gal-9, liver and spleen tissue sections (4 μm) from *Pb*ANKA-infected mice and uninfected controls were deparaffinized and rehydrated in distilled water. Heat-induced antigen retrieval was carried out in an 800-W microwave oven for 30 min. Endogenous peroxidase activity was blocked by incubation with 3 % hydrogen peroxide in methanol for 5 min at room temperature, then incubated with anti-Gal-9 Ab (Beijing Bioss Biological Co., Ltd, China) (1:400 dilutions) and anti-Tim-3 Ab (Wuhan Boster Biological Engineering Co., Ltd., China) (1:200 dilutions) overnight at 4 °C. Control sections were incubated with PBS without a primary antibody, and sections incubated with secondary antibodies only were used as isotype controls. Immunohistochemical staining was then detected with a SABC kit and developed with diaminobenzidine tetrahydrochloride (Zhongshan Goldenbridge Technology, Beijing, China). The sections were counterstained with hematoxylin and positive cells were identified by dark-brown staining. The numbers of positive cells in liver and spleen tissues were determined by microscopic examination and were measured by computer imaging, using software of Image Z1 (Sun Yat-sen University, China). The densities of positive cells were expressed as the numbers of cells per square millimeter. The number of cells in each field was determined under high power field as well as the area of each field (0.015066 mm^2).

Measurement of mRNA expression using quantitative real-time PCR (qRT-PCR)

Total RNA was extracted from about 100 mg of the livers and spleens of each group using an RNA Extraction Kit (TaKaRa) according to the manufacturer's protocol. The quality of total RNA was analyzed by running 5 µl of each RNA sample on a 1.0 % agarose gel stained with ethidium bromide. The quantity of total RNA was estimated by measuring the ratio of absorbance at 260 and 280 nm using a NanoDrop ND-1000 spectrophotometer (NanoDrop Technologies). First-strand cDNA was constructed from 1.0 µg of total RNA with oligo (dT) as primers using a PrimeScript 1st Strand cDNA Synthesis Kit (TaKaRa) following the manufacturer's protocol. cDNA was stored at −80 °C until use. To detect Tim-3, Gal-9, TNF-α, IL-1β, IL-4, IL-6, and IL-10 mRNA levels of the livers and spleens, qRT-PCR was performed using SYBR Green QPCR Master Mix (TaKaRa) according to the manufacturer's instructions. For liver and spleen parasite burdens, mRNA level of *Pb*ANKA 18S rRNA measured using qRT-PCR is shown as $-^{\triangle\triangle}Ct$ values. Primers are listed in Table 1. Briefly, a total of 10 µl reaction mixture contained 5.0 µl of SYBR® Premix Ex Taq™ (2×), 0.5 µl of each primer (10 pM), 3.0 µl of dH$_2$O, and 1.0 µl of cDNA (0.2 µg/µl). Amplification was pre-denaturized for 30 s at 95 °C followed by 43 cycles of 5 s at 95 °C and 20 s at 60 °C with a LightCycler® 480 instrument (Roche Diagnostics). Specific mRNA expression levels were normalized to that of the housekeeping gene, β-actin, and the results were expressed using a comparative threshold cycle (CT) value with the formula: $^{\triangle}CT = CT_{(gene\ of\ interest)} - CT_{(\beta-actin)}$. The relative expressions were then calculated using the formula $2^{-\triangle\triangle CT}$ compared to uninfected controls (Schmittgen and Livak 2008).

Statistical analysis

Results of experimental studies are reported as mean±standard deviation (mean±SD). Statistical analysis of the data was performed using Wilcoxon rank sum test, Student's *t* test, and one-way ANOVA followed by Bonferroni's multiple comparison test using SPSS software for Windows (version 19.0; SPSS, Inc., IL). All graphs were performed using GraphPad Prism software and a value of $P < 0.05$ was considered statistically significant.

Results

Malarial mouse model

After infection of 10^6 *Pb*ANKA-iRBCs, KM mice died between 7 and 20 days p.i. The parasitemia reached 62.61 to 78.63 % when deaths occurred at day 20 p.i. Tissue parasite burdens of the *Pb*ANKA-infected mice were detected using qRT-PCR. As shown in Fig. 1, the expressions of *Pb*ANKA 18S rRNA in livers and spleens of *Pb*ANKA-infected mice were increased with time after infection. Compared with day 5 p.i., the parasite burdens in the livers and spleens were significantly increased at days 10 ($P<0.05$), 15 ($P<0.001$), and 20 ($P<0.001$) p.i.; compared with day 10 p.i., the parasite

Table 1 Primer sequences of mouse target cytokines and housekeeping genes used for quantitative real-time polymerase chain reaction (qRT-PCR) assays

| Genes	Primer sequence (5′→3′)		References
P. berghei ANKA 18S	Forward primer Reverse primer	AAGCATTAAATAAAGCGAATACATCCTTAC GGAGATTGGTTTTGACGTTTATGTG	Mimche et al. (2015)
TNF-α	Forward primer Reverse primer	CCCTCACACTCAGATCATCTTCT GCTACGACGTGGGCTACAG	Zhao et al. (2011)
IL-10	Forward primer Reverse primer	AGCCGGGAAGACAATAACTG CATTTCCGATAAGGCTTGG	Jones et al. (2010)
IL-4	Forward primer Reverse primer	ACAGGAGAAGGGACGCCAT GAAGCCCTACAGACGAGCTCA	Jash et al. (2011)
IL-6	Forward primer Reverse primer	ACACATGTTCTCTGGGAAATCGT AAGTGCATCATCGTTGTTCATACA	Mimche et al. (2015)
IL-1β	Forward primer Reverse primer	GTGGCAGCTACCTGTGTCT GAGCCTGTAGTGCAGTTGTCT	Uri-Belapolsky et al. (2014)
Gal-9	Forward primer Reverse primer	GTTGTCCGAAACACTCAGAT ATATGATCCACACCGAGAAG	Reddy et al. (2011)
Tim-3	Forward primer Reverse primer	CCACGGAGAGAAATGGTTC CATCAGCCCATGTGGAAAT	Geng et al. (2006)
β-Actin	Forward primer Reverse primer	TGGAATCCTGTGGCATCCATGAAAC TAAAACGCAGCTCAGTAACAGTCCG	Jones et al. (2010)
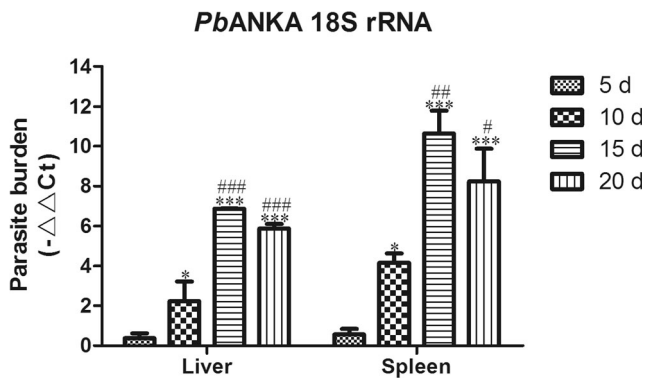
PbANKA 18S rRNA

Fig. 1 Parasite burdens in PbANKA-infected mice. For the liver and spleen parasite burdens, mRNA levels of PbANKA 18S rRNA measured using qRT-PCR are shown as $-\triangle\triangle Ct$ values. Values are means from triplicate measurements, and data are presented as mean±SD; two independent experiments were performed with three mice per group. *$P<0.05$, **$P<0.01$, and ***$P<0.001$ vs. 5 days p.i.; #$P<0.05$, ##$P<0.01$, and ###$P<0.001$ vs. 10 days p.i.

burdens in the livers and spleens were significantly increased at days 15 ($P<0.001$) and 20 ($P<0.001$ and $P<0.05$, respectively) p.i.

Liver and spleen tissue histopathology

To investigate the pathogenesis of PbANKA-infected mice, the tissues of livers and spleens were examined histologically. The livers and spleens from uninfected mice showed no morphological or structural abnormalities. However, the liver tissues of PbANKA-infected mice showed varying degrees of inflammation, liver sinusoidal expansion and swelling, atrophy and degeneration of hepatocytes, hypertrophy and hyperplasia of Kupffer cells (KCs) with hemozoin accumulation, and congestion of blood vessels with PRBCs at 5, 10, 15, and 20 days p.i. (Fig. 2a). The histopathology of spleen from PbANKA-infected mice at 5, 10, 15, and 20 days p.i. showed that the red and white pulp elements of spleens were enlarged and congested accompanied by loss of typical structure of the germinal center, and microvascular sequestrations of PRBCs and a large number of iRBCs deposit were present. The malarial pigments were deposited abundantly in the red pulp histiocytes and sinusoidal lining areas (Fig. 2b). Semi-quantitative score standard for severity was made based on pathological changes of the liver and spleen tissues in the times (Fig. 2c). Compared with day 5 p.i., there were significantly increased histological scores in the livers and spleens of PbANKA-infected mice at days 10, 15, and 20 p.i. ($P<0.001$); compared with day 10 p.i., there were significantly increased histological scores in the livers and spleens at days 15 and 20 p.i. ($P<0.001$), but the histological scores in the livers at day 20 p.i. was significantly lower than that at day 15 p.i. ($P<0.001$).

Immunohistochemical staining for Tim-3 and Gal-9 in the liver and spleen tissues

Immunohistochemical staining for Tim-3 and Gal-9 were detected to locate their expressions in the liver and spleen tissues of PbANKA-infected mice at all the times. Morphological or structural abnormalities were massively distorted, and numerous positive cells (brown) were dispersed in the sections of the livers (Fig. 3a, b) and spleens (Fig. 4a). As shown in Fig. 3c, compared with uninfected controls, there were significantly higher numbers of Tim-3- and Gal-9-positive cells in the livers at days 5, 10, 15, and 20 p.i. ($P<0.001$). Compared with day 5 p.i., there were significant higher numbers of Tim-3- and Gal-9-positive cells in the livers at days 10, 15, and 20 p.i. ($P<0.001$). Compared with day 10 p.i., there were significantly higher numbers of Tim-3- and Gal-9-positive cells in the livers at days 15 ($P<0.001$ and $P<0.05$, respectively) and 20 ($P<0.001$) p.i.; the numbers of Tim-3- and Gal-9-positive cells were significantly higher in the livers at day 20 p.i. ($P<0.001$) compared with that of day 15 p.i. As shown in Fig. 4b, compared with uninfected controls, there were significantly higher numbers of Tim-3- and Gal-9-positive cells in the spleens at days 5, 10, 15, and 20 p.i. ($P<0.001$). Compared with day 5 p.i., there were significantly higher numbers of Tim-3-positive cells in the spleens at day 10 p.i. ($P<0.001$) and significantly higher numbers of Tim-3- and Gal-9-positive cells at days 15 and 20 p.i. ($P<0.001$); compared with day 10 p.i., there were significantly lower numbers of Tim-3-positive cells but significantly higher numbers of Gal-9-positive cells in the spleens at day 15 p.i. ($P<0.001$) and significantly higher numbers of Gal-9-positive cells at day 20 p.i. ($P<0.001$); the positive cells of Tim-3 and Gal-9 in the spleens at day 20 p.i. were significantly higher than those at day 15 p.i. ($P<0.01$ and $P<0.001$, respectively). No positive results were observed in sections incubated with only secondary antibodies (goat IgG1), which were used as the negative controls.

Tim-3/Gal-9 mRNA expressions in the livers and spleens

The mRNA expressions of Tim-3 and Gal-9 in the livers and spleens of PbANKA-infected mice were determined using qRT-PCR to further confirm their presence. As shown in Fig. 5, compared with uninfected controls, Tim-3 mRNA levels in the livers of the PbANKA-infected mice were significantly increased at days 5 ($P<0.01$), 10 ($P<0.05$), 15 ($P<0.001$), and 20 ($P<0.001$) p.i.; the Tim-3 mRNA levels in the livers at day 20 p.i. were significantly higher than those at days 5, 10, and 15 p.i. ($P<0.001$). Compared with uninfected controls, Gal-9 levels in the
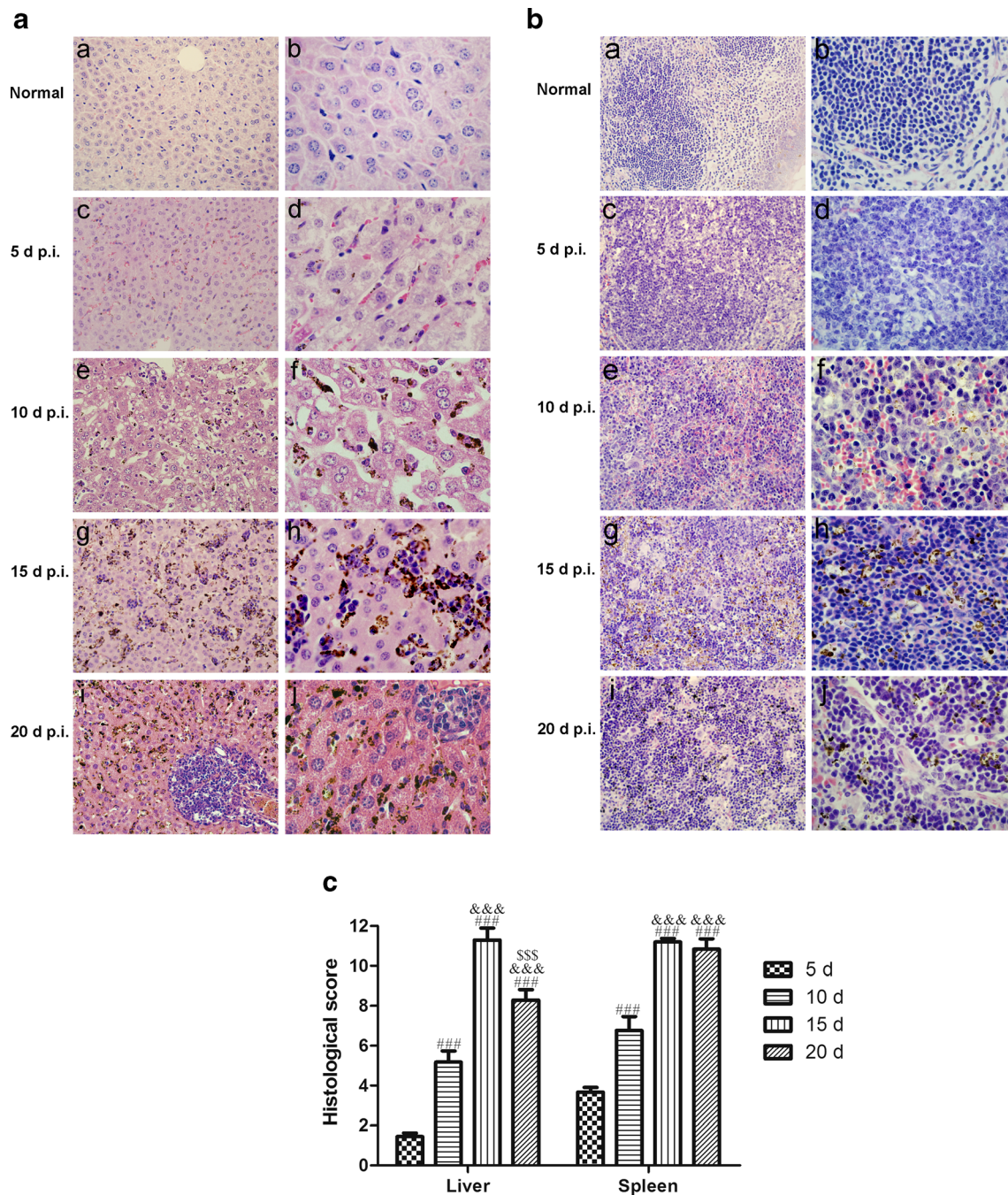
a

b

c

Fig. 2 Histopathological changes and semi-quantitative analysis of the liver and spleen tissues from *Pb*ANKA-infected KM mice. **a** Histopathological changes in the livers. Naïve mice, no histological alterations were observed (**a, b**); mice infected with *Pb*ANKA at days 5 (**c, d**), 10 (**e, f**), 15 (**g, h**), and 20 (**i, j**) p.i. Original magnification ×400 (**a, c, e, g, i**), ×1000 (**b, d, f, h, j**); H&E stain. **b** Histopathological changes in the spleens. Naïve mice, no histological alterations were observed (**a, b**); mice infected with *Pb*ANKA at days 5 (**c, d**), 10 (**e, f**), 15 (**g, h**), and 20 (**i, j**) p.i. Original magnification ×400 (**a, c, e, g, i**), ×1000 (**b, d, f, h, j**); H&E stain.

c Histological scores of the liver and spleen sections from different groups. Changes in histological appearance were assessed semi-quantitatively. Total grades ranged from 4 to 12, with 12 representing severe degeneration. Data are represented as mean ± SD. Significant differences between groups are analyzed using Wilcoxon rank sum test. [#]$P<0.05$, [##]$P<0.01$, and [###]$P<0.001$ vs. 5 days p.i.; [&]$P<0.05$, [&&]$P<0.01$, and [&&&]$P<0.001$ vs. 10 days p.i.; [$]$P<0.05$, [$$]$P<0.01$, and [$$$]$P<0.001$ vs. 15 days p.i.

livers of the *Pb*ANKA-infected mice were significantly increased at days 5 and 10 p.i. ($P<0.001$), while compared

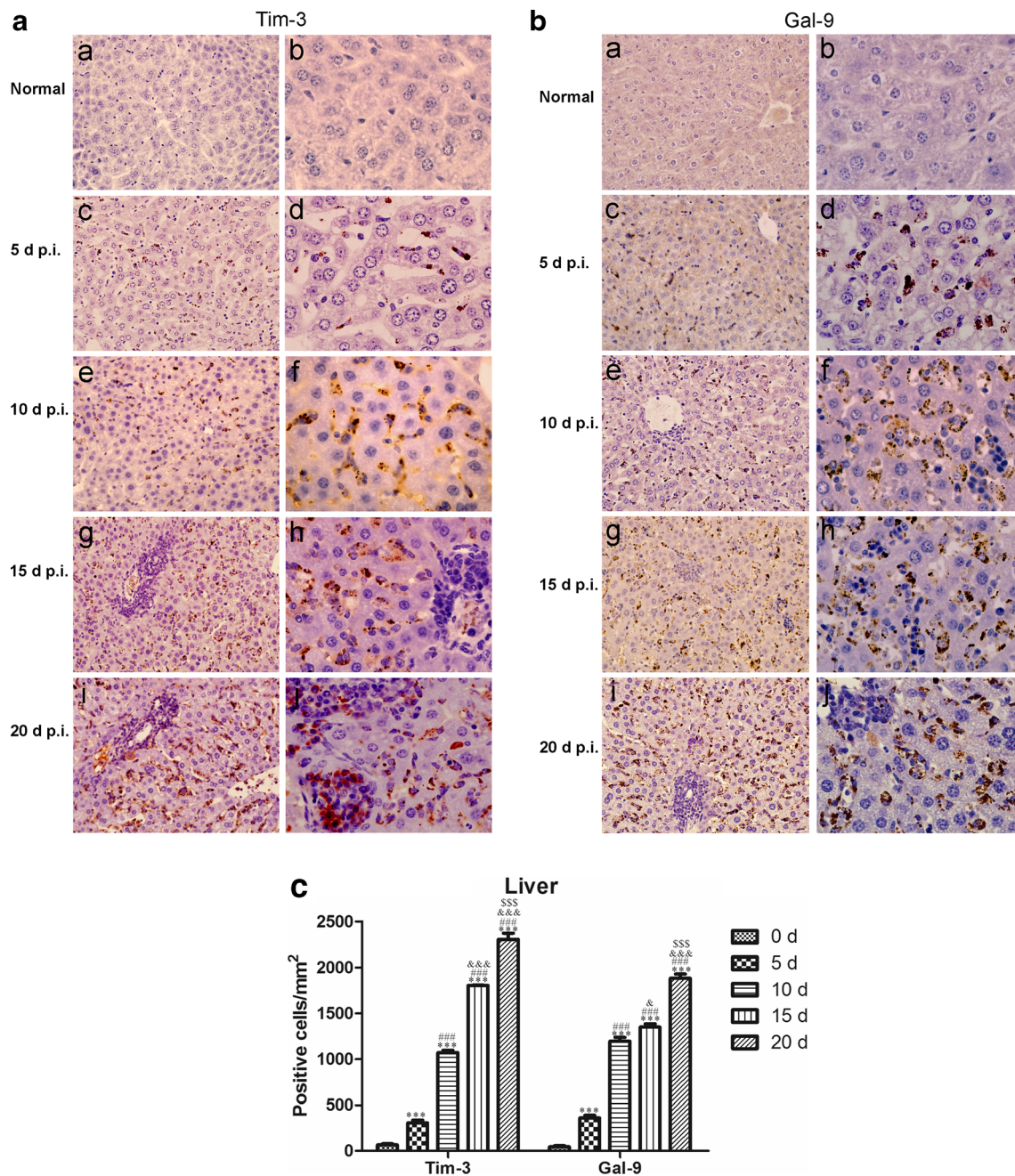with day 5 p.i., Gal-9 levels in the livers were significantly decreased at days 15 and 20 p.i. ($P<0.001$). Compared

Fig. 3 Immunohistochemical staining and morphometric analysis for Tim-3 and Gal-9 in the liver tissues of mice infected with *Pb*ANKA. Immunohistochemical staining of Tim-3 (**a**) and Gal-9 (**b**) in the livers. Naïve mice (**a, b**); mice infected with *Pb*ANKA at days 5 (**c, d**), 10 (**e, f**), 15 (**g, h**), and 20 (**i, j**) p.i. Original magnification ×400 (**a, c, e, g, i**), ×1000 (**b, d, f, h, j**). **c** Data for analyses of Tim-3 and Gal-9 in the livers; the density of positive cells was expressed as the number of cells per square millimeter. Data are presented as mean±SD; experiments were performed with three mice per group. *$P<0.05$, **$P<0.01$, and ***$P<0.001$ vs. control group; #$P<0.05$, ##$P<0.01$, and ###$P<0.001$ vs. 5 days p.i.; &$P<0.05$, &&$P<0.01$, and &&&$P<0.001$ vs. 10 days p.i.; $P<0.05$, $$$P<0.01$, and $$$$P<0.001$ vs. 15 days p.i.

with day 10 p.i., Gal-9 levels in the livers were significantly decreased at days 15 and 20 p.i. ($P<0.001$). Compared with uninfected controls, Tim-3 levels in the spleens of the *Pb*ANKA-infected mice were significantly decreased at days 5 and 15 p.i. ($P<0.001$), but the Gal-9 levels in the spleens were significantly increased at days 10 ($P<0.001$) and 15 ($P<0.05$) p.i.

Cytokine responses in the livers and spleens

To fully understand the immune responses in the experimental malarial mice, the cytokine levels were evaluated by measuring pro-inflammatory (IL-1β, IL-6, and TNF-α) and anti-inflammatory cytokine (IL-10 and IL-4) mRNA expressions in the livers and spleens of *Pb*ANKA-infected mice. As shown
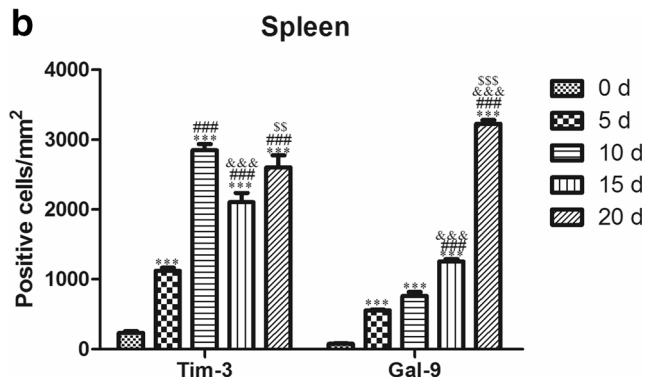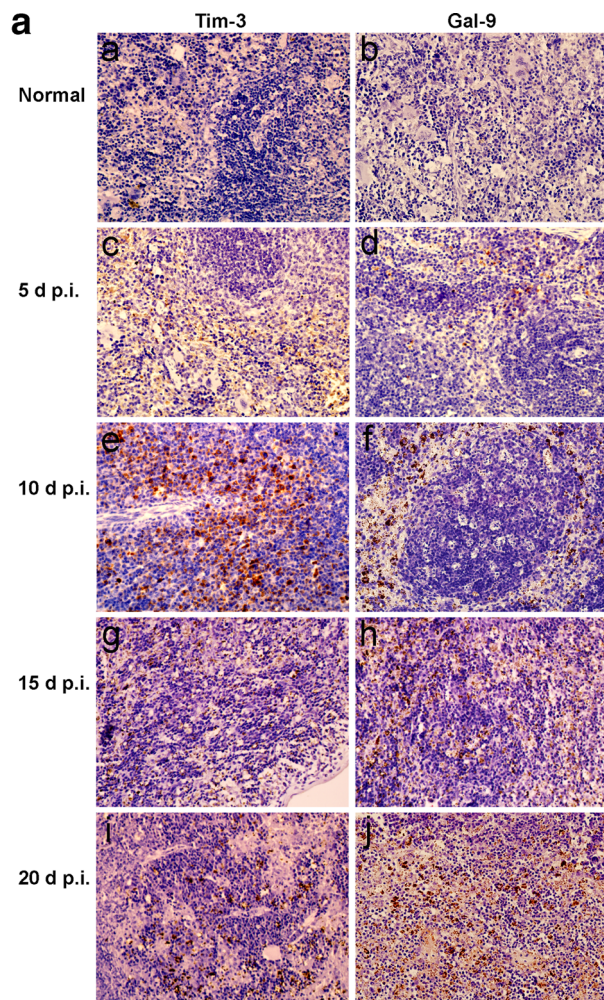
Fig. 4 Immunohistochemical staining and morphometric analysis for Tim-3 and Gal-9 in the spleen tissues of mice infected with PbANKA. **a** Immunohistochemical staining of Tim-3 (**a**, **c**, **e**, **g**, **i**) and Gal-9 (**b**, **d**, **f**, **h**, **j**) in the spleens. Naïve mice (**a**, **b**); mice infected with PbANKA at days 5 (**c**, **d**), 10 (**e**, **f**), 15 (**g**, **h**), and 20 (**i**, **j**) p.i.; Original magnification ×400. **b** Data for analyses of Tim-3 and Gal-9 in the spleens; the density of positive cells was expressed as the number of cells per square millimeter. Data are presented as mean±SD; experiments were performed with three mice per group. *$P<0.05$, **$P<0.01$, and ***$P<0.001$ vs. control group; #$P<0.05$, ##$P<0.01$, and ###$P<0.001$ vs. 5 days p.i.; &$P<0.05$, &&$P<0.01$, and &&&$P<0.001$ vs. 10 days p.i.; $$P<0.05$, $$$P<0.01$, and $$$P<0.001$ vs. 15 days p.i.
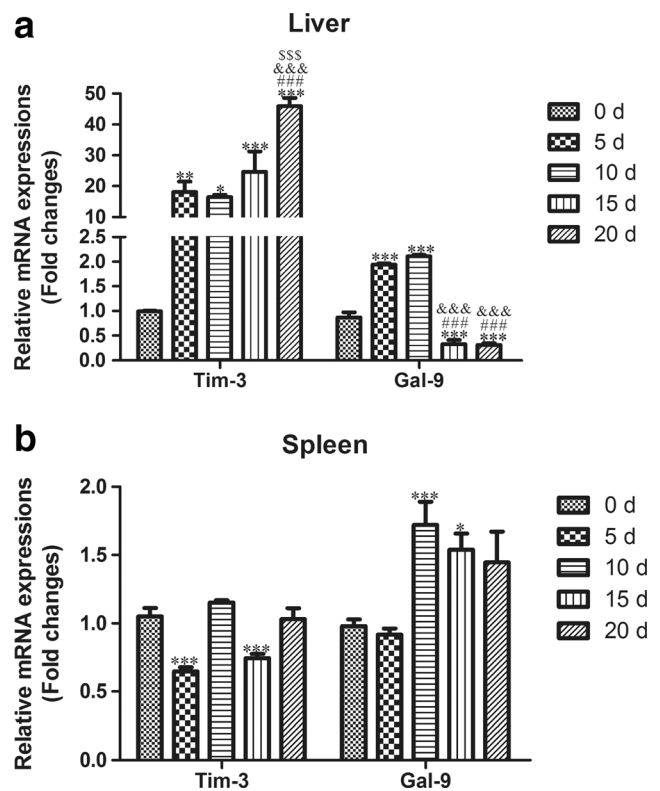

Fig. 5 Tim-3 and Gal-9 mRNA expressions in the livers and spleens of PbANKA-infected KM mice using qRT-PCR. Values are means from triplicate measurements, and data are presented as mean±SD; two independent experiments were performed with three mice per group. *$P<0.05$, **$P<0.01$, and ***$P<0.001$ vs. control group; #$P<0.05$, ##$P<0.01$, and ###$P<0.001$ vs. 5 days p.i.; &$P<0.05$, &&$P<0.01$, and &&&$P<0.001$ vs. 10 days p.i.; $$P<0.05$, $$$P<0.01$, and $$$P<0.001$ vs. 15 days p.i.

in Fig. 6, compared with uninfected controls, the proinflammatory cytokine mRNA levels of IL-1β in the livers of PbANKA-infected mice were significantly increased at days 15 ($P<0.001$) and 20 ($P<0.05$) p.i., and the IL-1β levels at day 15 p.i. were significant higher than that at day 20 p.i. ($P<0.05$); however, IL-1β levels in the spleens were significantly decreased at days 10 ($P<0.001$), 15 ($P<0.01$), and 20 ($P<0.001$) p.i. Compared with uninfected controls, the mRNA levels of IL-6 in both the livers and spleens were significantly increased at days 5 ($P<0.01$), 10 ($P<0.001$), 15 ($P<0.001$), and 20 ($P<0.001$) p.i., and the levels of IL-6 in the livers at day 15 p.i. were significantly higher than those at days 5 and 10 p.i. ($P<0.05$). Compared with day 5 p.i., the levels of IL-6 in the spleens were significantly increased at days 15 and 20 p.i. ($P<0.001$); compared with day 10 p.i., the mRNA levels of IL-6 in the spleens were significantly increased at days 15 and 20 p.i. ($P<0.05$). Compared with uninfected controls, the mRNA levels of TNF-α were significantly increased in the livers at days 10 ($P<0.05$), 15 ($P<0.001$), and 20 ($P<0.001$) p.i., while the levels of TNF-α in the livers at day 15 p.i. were significantly higher than that at day 10 p.i.

Fig. 6 Pro-inflammatory (IL-1β, IL-6, and TNF-α) and anti-inflammatory (IL-10 and IL-4) cytokine mRNA expressions in the livers and spleens of *Pb*ANKA-infected KM mice using qRT-PCR. Values are means from triplicate measurements, and data are presented as mean±SD; two independent experiments were performed with three mice per group. *$P<0.05$, **$P<0.01$, and ***$P<0.001$ vs. control group; #$P<0.05$, ##$P<0.01$, and ###$P<0.001$ vs. 5 days p.i.; &$P<0.05$, &&$P<0.01$, and &&&$P<0.001$ vs. 10 days p.i.; $$P<0.05$, $$P<0.01$, and $$$P<0.001$ vs. 15 days p.i.
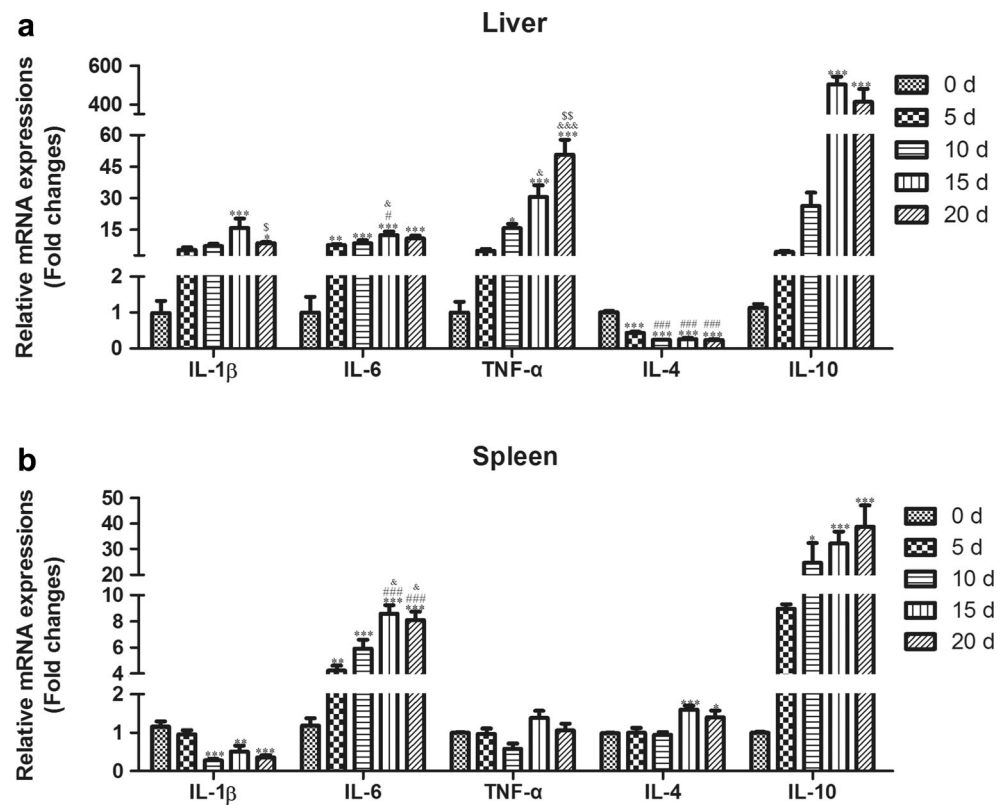
($P<0.05$) and that at day 20 p.i. were significantly higher than those at days 10 ($P<0.001$) and 15 ($P<0.01$) p.i. Compared with uninfected controls, the levels of IL-10 were significantly increased at days 15 and 20 p.i. ($P<0.001$) in the livers and significantly increased at days 10 ($P<0.05$), 15 ($P<0.001$), and 20 ($P<0.001$) p.i. in the spleens. Compared with uninfected controls, the levels of IL-4 were significantly decreased at days 5, 10, 15, and 20 p.i. ($P<0.001$) in the livers, while the levels of IL-4 were significantly increased at days 15 ($P<0.001$) and 20 ($P<0.05$) p.i. in the spleens.

Discussion

Murine malaria caused by *Pb*ANKA has been used as a valuable model of human malaria (Jennings et al. 1997; Helegbe et al. 2011). In this study, KM mice were i.p. inoculated with *Pb*ANKA-iRBCs and the immune responses in livers and spleens during the course were investigated. The observation of histopathological changes showed that hyperemia, malarial pigments, hyperplasia and hypertrophy of KCs, vacuolar degeneration and atrophy of hepatocytes, and microvascular congestion were in the liver tissues of *Pb*ANKA-infected mice; malarial pigments, red and white pulp elements enlarged and congested, lost the typical structure of germinal center, and microvascular sequestrated and iRBCs deposited were presented in the spleens. Our data obtained from *Pb*ANKA-infected KM outbred mice was similar to the results from severe *P. falciparum* malaria patients and *Pb*ANKA-infected ICR outbred mice reported (Fazalul Rahiman et al. 2013; Viriyavejakul et al. 2014), suggesting that this mouse model is helpful in the study of liver damage in erythrocytic stage of *Plasmodium* infection.

As liver can be an important target organ in malaria, studies have shown that liver injury can be developed during the erythrocyte stage of *P. berghei* infection in mice. Hepatocyte damage is associated with the advanced stages of *P. berghei* malarial infection, which lead to liver dysfunction (Rodríguez-Acosta et al. 1998). Liver damage during blood-stage malaria infection has also been modeled in mice using the *P. berghei* NK65 strain (Adachi et al. 2001, 2004; Findlay et al. 2010). Large numbers of infected erythrocytes pass through the spleen and liver. Phagocytic cells of both organs are involved in the uptake of infected erythrocytes and of free merozoites, which are released after rupture of their erythrocytic hosts (Singh et al. 2002). Assessment of parasite loads by qRT-PCR was performed in this study; our result showed that liver and spleen parasite burdens in *Pb*ANKA-infected mice were increased as time progressed. Parasites accumulated in tissue play a critical role in driving multi-organ pathology during *Pb*ANKA infection, and liver damage is a function of parasite burden in the liver (Haque et al. 2011).

The Tim-3/Gal-9 pathway plays a dual role in immunity. On one hand, it favors a pro-inflammatory response, induces

maturation of monocyte-derived dendritic cells, and, through this process, enhances Th1-type immune responses (Anderson et al. 2007). On the other hand, Gal-9 contributes to apoptosis of thymocytes and peripheral T cells, implicating a dual role of the Tim-3/Gal-9 axis in both T-cell maturation and negative regulation of T-cell-mediated immune reactions (Sánchez-Fueyo et al. 2003; Zhu et al. 2011). The Tim-3/Gal-9 signaling axis mediates T-cell dysfunction and predicts poor prognosis in patients with HBV-associated HCC (Li et al. 2012). The relevance of Tim-3/Gal-9 signaling axis is maintaining a balanced local immune microenvironment in the liver. As the natural ligand for Tim-3, Gal-9 is widely distributed throughout various tissues, being particularly abundant in the liver (Wada and Kanwar 1997), which is among the most potent immunologic organs (Rosen. 2008). Dysregulation of this axis can lead to a chronic inflammatory liver disorder (Bacigalupo et al. 2013). Blockade of the Tim-3/Gal-9 pathway exacerbated local inflammation and liver damage (Uchida et al. 2010), suggesting the importance of Tim-3/Gal-9 signaling in the maintenance of liver homeostasis and controlling dysregulated liver immune response. In the present study, our data showed significantly increased numbers of Tim-3- and Gal-9-positive cells in both the livers and spleens of *Pb*ANKA-infected mice at days 5, 10, 15, and 20 p.i. using immunohistochemical staining; detection of Tim-3/Gal-9 mRNA expressions in livers and spleens showed that Tim-3 levels were significantly increased in the livers of *Pb*ANKA-infected mice, and Gal-9 levels were significantly increased in both livers and spleens after infection. It has been reported that patients with non-viral liver disease had intermediate levels of Gal-9, suggesting it may play an important role in the hepatic immune response (Vollmar and Menger 2009). Gal-9 is a pro-inflammatory factor that promotes tissue inflammation (Anderson et al. 2007), has a major role in limiting the immune response (Anderson and Anderson 2006), but also enhances Th1 immune responses (Klibi et al. 2009). In this study, we demonstrated that *Pb*ANKA infection caused the increase of Tim-3 and Gal-9 expressions in the livers and spleens of *Pb*ANKA-infected mice. Although the regulatory mechanisms were unknown, our data indicates that Tim-3/Gal-9 may be involved in *Pb*ANKA-induced liver pathology.

Cytokines are important immune mediators and regulators with both protective and pathogenic functions in malaria (Engwerda et al. 2005; Good et al. 2005), in which IFN-γ and TNF-α help T cells and Tc cells proliferation, differentiation, and maturation, mainly promoting the cell-mediated immune response, which is extremely important to the immunity of malaria infection in macrophages; IL-4 and IL-10 help B-cell proliferation and maturation, and promote antibody generation, mainly amplifying the immune response mediated by the antibodies. Gal-9 has pleiotropic roles and may represent a novel therapeutic target in patients with viral or inflammatory diseases of the liver (Zhu et al. 2005). In this study, our

results showed that pro-inflammatory (IL-1β, IL-6, and TNF-α) and anti-inflammatory (IL-10) cytokines were overexpressed in the livers, and IL-4, IL-6, and IL-10 were overexpressed in the spleens after infection. KC-derived Gal-9 induces the secretion of an array of pro-inflammatory mediators (TNF-α, IL-1β, and IFN-γ) that can further amplify the immunopathology associated with HCV (Mengshol et al. 2010). Additional modulators of Gal-9 include IL-1β and IL-5 in astrocytes (Yoshida et al. 2001) and eosinophils (Saita et al. 2002), respectively. All those implicate that Tim-3/Gal-9 as a key regulator in inflammatory pathways within the liver leads to injury.

In conclusion, *Pb*ANKA infection upregulates the expressions of Tim-3 and Gal-9 in the liver of *Pb*ANKA-infected KM mice, and may impact pro-inflammatory and anti-inflammatory cytokines' immune response during the *Pb*ANKA infection. Our data may provide evidence for the prevention and treatment of malaria infection through Tim-3/Gal-9 signal pathway. However, the precise immune mechanisms induced by *Plasmodium* need further study.

References

Adachi K, Tsutsui H, Kashiwamura SI, Seki E, Nakano H, Takeuchi O, Takeda K, Okumura K, Van Kaer L, Okamura H, Akira S, Nakanishi K (2001) *Plasmodium berghei* infection in mice induces liver injury by an IL-12- and Toll-like receptor/myeloid differentiation factor 88-dependent mechanism. J Immunol 167(10):5928–5934

Adachi K, Tsutsui H, Seki E, Nakano H, Takeda K, Okumura K, Van Kaer L, Nakanishi K (2004) Contribution of CD1d-unrestricted hepatic DX5$^+$ NKT cells to liver injury in *Plasmodium berghei*-parasitized erythrocyte-injected mice. Int Immunol 16(6):787–798

Anand AC, Puri P (2005) Jaundice in malaria. J Gastroenterol Hepatol 20(9):1322–1332

Anderson AC, Anderson DE (2006) TIM-3 in autoimmunity. Curr Opin Immunol 18(6):665–669

Anderson AC, Anderson DE, Bregoli L, Hastings WD, Kassam N, Lei C, Chandwaskar R, Karman J, Su EW, Hirashima M, Bruce JN, Kane LP, Kuchroo VK, Hafler DA (2007) Promotion of tissue inflammation by the immune receptor Tim-3 expressed on innate immune cells. Science 318(5853):1141–1143

Bacigalupo ML, Manzi M, Rabinovich GA, Troncoso MF (2013) Hierarchical and selective roles of galectins in hepatocarcinogenesis, liver fibrosis and inflammation of hepatocellular carcinoma. World J Gastroenterol 19(47):8831–8849

Berrocal Almanza LC, Muñoz M, Kühl AA, Kamradt T, Heimesaat MM, Liesenfeld O (2013) Tim-3 is differently expressed in genetically susceptible C57BL/6 and resistant BALB/c mice during oral infection with *Toxoplasma gondii*. Eur J Microbiol Immunol (Bp) 3(3): 211–221

Engwerda C, Belnoue E, Grüner AC, Rénia L (2005) Experimental models of cerebral malaria. Curr Top Microbiol Immunol 297: 103–143

Fazalul Rahiman SS, Basir R, Talib H, Tie TH, Chuah YK, Jabbarzare M, Chong WC, Mohd Yusoff MA, Nordin N, Yam MF, Abdullah WO, Abdul Majid R (2013) Interleukin-27 exhibited anti-inflammatory activity during Plasmodium berghei infection in mice. Trop Biomed 30(4):663–680

Findlay EG, Greig R, Stumhofer JS, Hafalla JC, de Souza JB, Saris CJ, Hunter CA, Riley EM, Couper KN (2010) Essential role for IL-27 receptor signaling in prevention of Th1-mediated immunopathology during malaria infection. J Immunol 185(4):2482–2492

Geng H, Zhang GM, Li D, Zhang H, Yuan Y, Zhu HG, Xiao H, Han LF, Feng ZH (2006) Soluble form of T cell Ig mucin 3 is an inhibitory molecule in T cell-mediated immune response. J Immunol 176(3): 1411–1420

Good MF, Xu H, Wykes M, Engwerda CR (2005) Development and regulation of cell-mediated immune responses to the blood stages of malaria: implications for vaccine research. Annu Rev Immunol 23:69–99

Haque A, Best SE, Amante FH, Ammerdorffer A, de Labastida F, Pereira T, Ramm GA, Engwerda CR (2011) High parasite burdens cause liver damage in mice following Plasmodium berghei ANKA infection independently of CD8($^+$) T cell-mediated immune pathology. Infect Immun 79(5):1882–1888

Helegbe GK, Yanagi T, Senba M, Huy NT, Shuaibu MN, Yamazaki A, Kikuchi M, Yasunami M, Hirayama K (2011) Histopathological studies in two strains of semi-immune mice infected with Plasmodium berghei ANKA after chronic exposure. Parasitol Res 108(4):807–814

Jash A, Kwon HK, Sahoo A, Lee CG, So JS, Kim J, Oh YK, Kim YB, Im SH (2011) Topical application of porcine placenta extract inhibits the progression of experimental contact hypersensitivity. J Ethnopharmacol 133(2):654–662

Jennings VM, Actor JK, Lal AA, Hunter RL (1997) Cytokine profile suggesting that murine cerebral malaria is encephalitis. Infect Immun 65(11):4883–4887

Jones LA, Roberts F, Nickdel MB, Brombacher F, McKenzie AN, Henriquez FL, Alexander J, Roberts CW (2010) IL-33 receptor (T1/ST2) signaling is necessary to prevent the development of encephalitis in mice infected with Toxoplasma gondii. Eur J Immunol 40(2):426–436

Klibi J, Niki T, Riedel A, Pioche-Durieu C, Souquere S, Rubinstein E, Le Moulec S, Guigay J, Hirashima M, Guemira F, Adhikary D, Mautner J, Busson P (2009) Blood diffusion and Th1-suppressive effects of galectin-9-containing exosomes released by Epstein-Barr virus-infected nasopharyngeal carcinoma cells. Blood 113(9):1957–1966

Li H, Wu K, Tao K, Chen L, Zheng Q, Lu X, Liu J, Shi L, Liu C, Wang G, Zou W (2012) Tim-3/galectin-9 signaling pathway mediates T-cell dysfunction and predicts poor prognosis in patients with hepatitis B virus-associated hepatocellular carcinoma. Hepatology 56(4):1342–1351

Li Z, Ju Z, Frieri M (2013) The T-cell immunoglobulin and mucin domain (Tim) gene family in asthma, allergy, and autoimmunity. Allergy Asthma Proc 34(1):e21–e26

Mengshol JA, Golden-Mason L, Arikawa T, Smith M, Niki T, McWilliams R, Randall JA, McMahan R, Zimmerman MA, Rangachari M, Dobrinskikh E, Busson P, Polyak SJ, Hirashima M, Rosen HR (2010) A crucial role for Kupffer cell-derived galectin-9 in regulation of T cell immunity in hepatitis C infection. PLoS One 5(3):e9504

Mimche PN, Brady LM, Bray CF, Mimche SM, Thapa M, King TP, Quicke K, McDermott CD, Lee CM, Grakoui A, Morgan ET, Lamb TJ (2015) The receptor tyrosine kinase EphB2 promotes hepatic fibrosis in mice. Hepatology Mar 17

Murthy GL, Sahay RK, Sreenivas DV, Sundaram C, Shantaram V (1998) Hepatitis in falciparum malaria. Trop Gastroenterol 19(4):152–154

Reddy PB, Sehrawat S, Suryawanshi A, Rajasagi NK, Mulik S, Hirashima M, Rouse BT (2011) Influence of galectin-9/Tim-3 interaction on herpes simplex virus-1 latency. J Immunol 187(11):5745–5755

Rodríguez-Acosta A, Finol HJ, Pulido-Méndez M, Márquez A, Andrade G, González N, Aguilar I, Girón ME, Pinto A (1998) Liver ultrastructural pathology in mice infected with Plasmodium berghei. J Submicrosc Cytol Pathol 30(2):299–307

Rosen HR (2008) Transplantation immunology: what the clinician needs to know for immunotherapy. Gastroenterology 134(6):1789–1801

Saita N, Goto E, Yamamoto T, Cho I, Tsumori K, Kohrogi H, Maruo K, Ono T, Takeya M, Kashio Y, Nakamura K, Hirashima M (2002) Association of galectin-9 with eosinophil apoptosis. Int Arch Allergy Immunol 128:42–50

Sánchez-Fueyo A, Tian J, Picarella D, Domenig C, Zheng XX, Sabatos CA, Manlongat N, Bender O, Kamradt T, Kuchroo VK, Gutiérrez-Ramos JC, Coyle AJ, Strom TB (2003) Tim-3 inhibits T helper type 1-mediated auto- and alloimmune responses and promotes immunological tolerance. Nat Immunol 4(11):1093–1101

Schmittgen TD, Livak KJ (2008) Analyzing real-time PCR data by the comparative C (T) method. Nat Protoc 3(6):1101–1108

Singh R, Kashiwamura S, Rao P, Okamura H, Mukherjee A, Chauhan V (2002) The role of IL-18 in blood-stage immunity against murine malaria Plasmodium yoelii 265 and Plasmodium berghei ANKA. J Immunol 168(9):4674–4681

Tang ZH, Liang S, Potter J, Jiang X, Mao HQ, Li Z (2013) Tim-3/galectin-9 regulate the homeostasis of hepatic NKT cells in a murine model of nonalcoholic fatty liver disease. J Immunol 190(4):1788–1796

Uchida Y, Ke B, Freitas MC, Yagita H, Akiba H, Busuttil RW, Najafian N, Kupiec-Weglinski JW (2010) T-cell immunoglobulin mucin-3 determines severity of liver ischemia/reperfusion injury in mice in a TLR4-dependent manner. Gastroenterology 139:2195–2206

Uri-Belapolsky S, Shaish A, Eliyahu E, Grossman H, Levi M, Chuderland D, Ninio-Many L, Hasky N, Shashar D, Almog T, Kandel-Kfir M, Harats D, Shalgi R, Kamari Y (2014) Interleukin-1 deficiency prolongs ovarian lifespan in mice. Proc Natl Acad Sci U S A 111(34):12492–12497

Viriyavejakul P, Khachonsaksumet V, Punsawad C (2014) Liver changes in severe Plasmodium falciparum malaria: histopathology, apoptosis and nuclear factor kappa B expression. Malar J 13:106

Vollmar B, Menger MD (2009) The hepatic microcirculation: mechanistic contributions and therapeutic targets in liver injury and repair. Physiol Rev 89(4):1269–1339

Wada J, Kanwar YS (1997) Identification and characterization of galectin-9, a novel beta-galactoside-binding mammalian lectin. J Biol Chem 272(9):6078–6086

Whitten R, Milner DA Jr, Yeh MM, Kamiza S, Molyneux ME, Taylor TE (2011) Liver pathology in Malawian children with fatal encephalopathy. Hum Pathol 42(9):1230–1239

WHO (2010) Guideline for the treatment of malaria, 2nd ed

Yoshida H, Imaizumi T, Kumagai M, Kimura K, Satoh C, Hanada N, Fujimoto K, Nishi N, Tanji K, Matsumiya T, Mori F, Cui XF, Tamo W, Shibata T, Takanashi S, Okumura K, Nakamura T, Wakabayashi K, Hirashima M, Sato Y, Satoh K (2001) Interleukin-1beta stimulates galectin-9 expression in human astrocytes. Neuroreport 12: 3755–3758

Zhao J, Endoh I, Hsu K, Tedla N, Endoh Y, Geczy CL (2011) S100A8 modulates mast cell function and suppresses eosinophil migration in acute asthma. Antioxid Redox Signal 14(9):1589–1600

Zhu C, Anderson AC, Schubart A, Xiong H, Imitola J, Khoury SJ, Zheng XX, Strom TB, Kuchroo VK (2005) The Tim-3 ligand galectin-9 negatively regulates T helper type 1 immunity. Nat Immunol 6(12): 1245–1252

Zhu C, Anderson AC, Kuchroo VK (2011) TIM-3 and its regulatory role in immune responses. Curr Top Microbiol Immunol 350:1–15